PERGAMON

Deep-Sea Research II 45 (1998) 2599–2618

DEEP-SEA RESEARCH
PART II

Patterns of event and chronic hydrothermal venting following a magmatic intrusion: new perspectives from the 1996 Gorda Ridge eruption

Edward T. Baker*

National Oceanic and Atmospheric Administration, Pacific Marine Environmental Laboratory, 7600 Sand Point Way N.E., Seattle, WA 98115-0070, USA

Received 1 May 1997; accepted 12 July 1997

Abstract

The remote detection of a seismic swarm on the northern Gorda Ridge on 28 February 1996 prompted a three-cruise response effort to investigate event and chronic hydrothermal discharge associated with a dike intrusion. The GR1 cruise reached the northern Gorda only 10 days after seismicity began and discovered a 15 km-diameter event plume, EP96A, centered between depths 1800 and 2800 m above the shallowest portion of the axial valley axis ($\sim$3100 m). One month later, GR2 returned and found only a weak, near-bottom chronic plume at the EP96A site. A few kilometers to the south, however, GR2 mapped a distinctly different chronic plume ($\sim$2500–2900 m depth) as well as the edge of a second event plume, EP96B ($\sim$1800–2400-m depth), above the western wall of the axial valley. EP96B was seeded with a neutrally buoyant float, which traveled 10 net km to the northwest before surfacing on 10 June at the start of GR3. Mapping around the float location fully revealed EP96B, a 10 km diameter plume with a heat content $\sim$25% that of EP96A. Extensive observations within the axial valley determined that chronic venting was effectively exhausted within three months. Models seeking to explain the perturbation of hydrothermal venting by a dike intrusion and eruption must satisfy several criteria generalized from this and previous events: (1) venting begins (or increases) with the intrusion/eruption and declines exponentially afterwards; (2) the time scale of the post-intrusion decline varies within and among sites; (3) the discharge of multiple event plumes is common; (4) an existing high-temperature vent field may not be necessary or even conducive to event plume formation; and (5) the ratio of total chronic to event discharge varies among intrusion events. © 1999 Published by Elsevier Science Ltd. All rights reserved.

*Tel.: 206 526 6251; fax: 206 526 6054; e-mail: baker@pmel.noaa.gov.

0967-0645/99/$ – see front matter © 1999 Published by Elsevier Science Ltd. All rights reserved.
PII: S0967-0645(98)00085-X

1. Introduction

The discovery of event plumes (or megaplumes) over the Juan de Fuca Ridge (JDFR) in 1986 (Baker et al., 1987a) and 1987 (Baker et al., 1989) introduced a new process affecting seafloor hydrothermal systems: instantaneous perturbation by volcanic activity. The first opportunity to study the immediate aftermath of such an event came unexpectedly in 1991, when the submersible *Alvin* arrived at 9.8°N on the East Pacific Rise (EPR) only days after an eruption (Haymon et al., 1993). Submersible observations documented new lava flows and invigorated venting, but a lack of systematic water column sampling precluded a vent-field-scale summary of the discharge magnitude and variability. The advent of real-time acoustical monitoring of mid-ocean ridges in 1993 (Fox, 1995, and references therein) transformed the study of magmatically perturbed hydrothermal venting from fortuitous to systematic, at least in the northeast Pacific. Remote detection and rapid field response to magmatic events have facilitated increasingly precise assessments of the relative magnitude and temporal variability of instantaneous event plumes and the longer-lasting chronic hydrothermal discharge that follows. The systematic study of event and chronic plumes at the JDFR CoAxial eruption site from 1993 to 1996 revealed that multiple event plumes could arise from a single dike intrusion episode (Baker et al., 1995), that event plumes might represent only a minor portion of the total hydrothermal discharge associated with an intrusion, and that the magnitude of the discharge declined exponentially from its enhanced level immediately following the intrusion (Baker et al., 1998).

The second magmatic intrusion detected and rapidly responded to in the northeast Pacific began on the northern Gorda Ridge on February 28, 1996 (Fox and Dziak, 1998). Seismicity associated with this event lasted about three weeks and prompted a field response that included several cruises staffed by a varying group of investigators collectively called the Gorda Ridge Event Assessment Team (GREAT). This paper summarizes the physical characteristics of the event and chronic plumes found during the first three response cruises, and compares the results to previous events. I then use this collective information to generalize our present understanding of the generation of event plumes and their relationship to subsequent chronic discharge at the event location.

2. Background and methods

2.1. Geologic and hydrothermal setting

The Gorda Ridge is a slow- to intermediate-rate spreading center lying within 300 km of the coast of northern California and southern Oregon (Fig. 1). The northernmost segment (North Gorda) extends 68 km south from the Blanco Fracture Zone and is bisected by a deep (600–1400 m), wide ($\sim$17 km at the top of the valley walls) axial valley bathymetrically characteristic of a slow-spreading ridge, even though the full-spreading rate has been $\sim$55 km My^{-1} since at least 4 m.y. B.P.

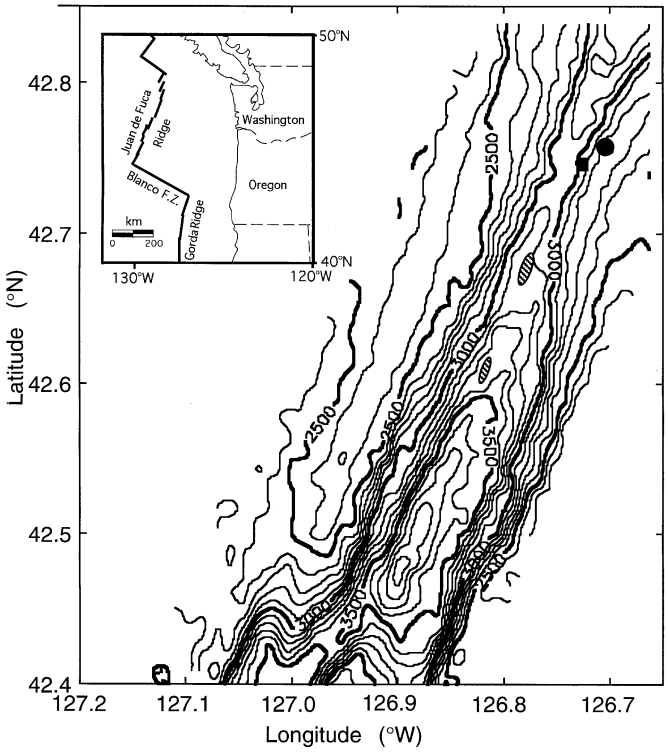

Fig. 1. Bathymetry of the northern Gorda Ridge. Cross-hatched ovals show approximate location of recent topographic anomalies near 42.67° and 42.61°N; the northernmost anomaly corresponds to a new lava flow mapped during the GR2 cruise (Chadwick et al., 1998). Solid square marks the location of the GR14 hydrothermal plume discovered in 1985 (Baker et al., 1987). Solid circle marks site of the Sea Cliff hydrothermal field discovered in 1988 (Rona et al., 1990).

(Riddihough, 1980). Hydrothermal plumes indicative of active venting were first discovered on this segment in May 1985 at two sites (Baker et al., 1987b): GR15, 42.95°N, 126.55°W, and GR14, 42.763°N, 126.730°W. At the GR14 site, close to the 1996 eruption location, plume anomalies in May 1985 reached a maximum at a depth of 2700 m and extended to the bottom at 3000 m. A follow-up cruise in August 1985 (Collier and Baker, 1990) found plume maxima between 2300 and 2700 m, significantly shallower than in May. As the Sea Cliff hydrothermal field (42.755°N, 126.708°W) was eventually found on the eastern valley wall at a depth of ~2700 m in 1988 (Rona et al., 1990), the deep plumes found in May 1985 must have originated at a different, deeper hydrothermal site. A third cruise in 1986 found no significant plume signals around the GR14 site (Collier and Baker, 1990), implying that discharge in the GR14 area was weak or intermittent or both. No water column observations were made within the axial valley of the northern Gorda Ridge between 1986 and 1996.

On February 28, 1996, the NOAA/VENTS T-phase monitoring program detected the onset of intense seismicity along the northern Gorda Ridge (Fox and Dziak, 1998). Acoustic signals were initially distributed between about 42.75°N and 42.50°N, became concentrated around 42.60°N by March 11, and ended by March 20. Both the level and duration of the seismicity were comparable to the 1993 CoAxial dike intrusion (Dziak et al., 1995) that generated at least three event plumes and two new hydrothermal fields. Analysis of the pattern of seismicity suggests that the Gorda Ridge event also produced a lateral dike intrusion starting near 42.75°N on March 1 and progressing to 42.45°N within 24 hours (Fox and Dziak, 1998). This hypothesis was confirmed by subsequent camera tows that discovered a new lava flow extending from 42.665°N to 42.688°N and centered at 126.78°W, just west of the valley axis (Fig. 1; Chadwick et al., 1998). Repeat swath-mapping also suggests a second, smaller, eruption from 42.605°N to 42.615°N and centered at 126.82°W, just north of a prominent seamount on the axial valley axis (Fig. 1; Chadwick et al., 1998). This second flow has not yet been verified.

2.2. Response history and methods

The GR1 cruise used the NOAA ship *McArthur* and was able to work at the Gorda Ridge for less than three days (2000 9 March–0600 12 March UTC) due to ship time limitations and bad weather. Operations on GR1 were limited to vertical CTD/optical (CTDO) casts. Based on the success of this cruise, the UNOLS ship *Wecoma* conducted GR2 from 0600 7 April to 0100 16 April (UTC). Operations included CTDO tows and casts, camera tows, and a RAFOS float deployment. Finally, the NOAA ship *Discoverer* undertook a series of CTDO tows and casts during GR3 from 1200 11 June to 0300 17 June (UTC).

All CTDO casts used a high-precision Sea Bird 911plus CTD, a Sea Tech light-scattering sensor (LSS), and a 20-bottle rosette. The Sea Tech LSS senses backscattered light from two modulated 880 nm light-emitting diodes. Temperature accuracy was better than 0.001°C; salinity accuracy, based on extensive comparisons with water samples run on an Autosal, was typically better than 0.0005; and LSS resolution was 0.0005 V (0.01% full scale). For tow-yos the CTDO package follows a sawtooth path through the water column as the winch continuously pays in and out while the ship steams steadily ahead at a speed of $\sim$2.5–3.5 km h^{-1}. The sawtooth wavelength varied with the water depth and was typically 0.5–2 km.

The hydrothermal temperature anomaly ($\Delta\theta$) is calculated for each depth z from the expression

$$\Delta\theta(z) = \theta(z) - (k\sigma_\theta(z) + b), \tag{1}$$

where $\theta(z)$ is potential temperature; $\sigma_\theta(z)$ is potential density; and k and b are regression coefficients for a fit of θ as a function of σ_θ within a few hundred meters above the neutrally buoyant plume. Small temperature anomalies caused by active hydrothermal venting can be difficult to distinguish from changes in the σ_θ vs. θ trend caused by long-term geothermal heating in the deep, confined basin of the North Gorda segment. Because the LSS measurement is relative rather than absolute and

differs slightly among individual instruments, I use an LSS anomaly (Δn) defined as the increase over ambient water immediately above the hydrothermal plume layer. The beam attenuation anomaly (Δc) can be estimated from Δn using the function

$$\Delta c \approx 0.5\Delta n \tag{2}$$

based on a least-squares regression ($r^2 = 0.955$) of LSS and transmissometer data from earlier hydrothermal plume cruises (Baker and Urabe, 1996; Baker et al., 1998).

Temperature and optical anomalies were calculated from despiked 1 Hz CTDO data averaged into 15 s blocks. The data were gridded at a vertical scale of 50 m and a horizontal scale of 1 km, and plume contours computed using a universal kreiging algorithm (Davis, 1987).

3. Time-series sampling

3.1. GR1

GR1 began with a series of vertical CTDO casts northward up the axial valley, starting at 42.438°N, 126.925°W (Fig. 2A). Although the depth of the valley floor varies from ~3900 m in the south to ~3000 m at 42.75°N, casts were limited to a depth of 2900 m by the available wire. No obvious hydrothermal indications were encountered until station GR1-V7, where intense $\Delta\theta$ and Δn signals were present from 1800 m to the cast bottom (Fig. 3A). Subsequent mapping defined event plume EP96A extending about 15 km along-axis and at least 8 km cross-axis between ~1800 and ~2700 m depth. The maximum $\Delta\theta$ observed in EP96A was ~0.12°C, only about half the maximum in event plumes at Cleft in 1986 (Baker et al., 1987a) and CoAxial in 1993 (Baker et al., 1995). Multiple maxima at different depths indicate that EP96A was fed by a variety of fluid releases of varying buoyancy, and that its formation was recent enough to have precluded homogenization by internal mixing. In fact, cast GR1-V8 sampled a small layer with a density inversion and an anomalous particle minimum indicative of a buoyant water parcel in which hydrothermal particle precipitation was only commencing. Extraordinarily high concentrations of H_2 at GR1-V7 and GR1-V8 confirm the youth of EP96A (Kelley et al., 1998). Our depth limitation of 2900 m prevented a sampling of chronic plumes beneath EP96A, although a weak plume layer centered around 2700 m on GR1-V7 and GR1-V8 (Fig. 3) may have been a chronic plume (Kelley et al., 1998; Massoth et al., 1998).

To inventory the hydrothermal heat contained in EP96A, the 1 km by 0.5 km grid used to construct the $\Delta\theta$ contours in Fig. 3 was rotated about the vertical axis of the plume to produce a suite of tori. The hydrothermal heat Q within any torus is given by

$$Q = CA\Delta\theta\,\rho\,C_p, \tag{3}$$

where C is the integral path length around a given torus, A is the vertical area (typically 0.05 km^2) of the grid cell, and ρC_p is the fluid heat capacity (4×10^6 J m^{-3} °C^{-1}). The sum of the tori gives the total hydrothermal heat $\sum Q$ within the 0.01°C $\Delta\theta$ contour as 2.1×10^{16} J (Table 1). This estimate has a high uncertainty, given the

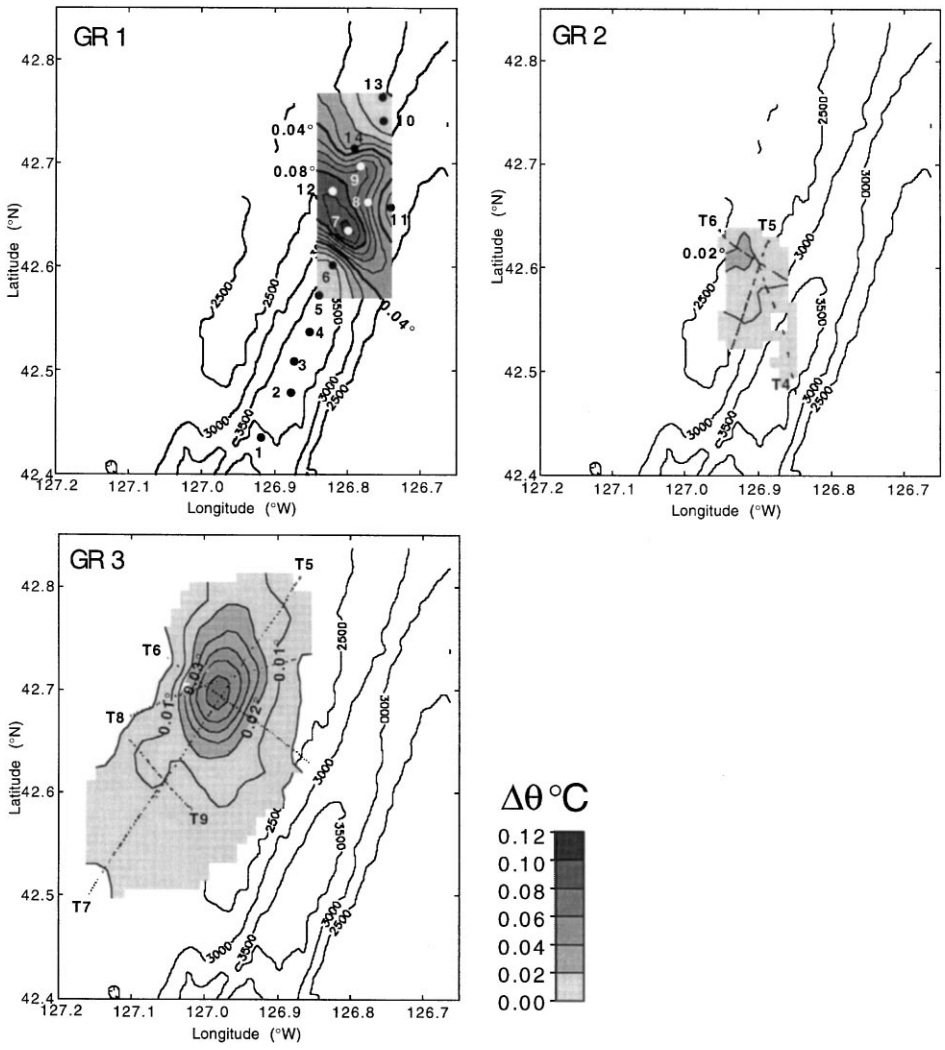

Fig. 2. Plan views of event plumes as a depth horizon of ~2100 m as defined by hydrothermal temperature anomalies mapped during the GR1, 2, and 3 cruises. Contour intervals of 0.01°C are plotted over the shade intervals of 0.02°C. Locations of vertical casts (GR1) and tow paths (GR2 and 3) also shown. True shape of the GR1 plume (EP96A) is uncertain owing to the relatively sparse data coverage.

non-symmetric internal structure of EP96A and the lack of a dense sampling grid normally provided by a tow-yo transect.

There is no evidence that the plumes mapped during GR1 were directly associated with the Sea Cliff hydrothermal field. Casts GR1-V10 and GR1-V13, well north of EP96A but bracketing the original GR 14 location, detected a slight plume between 2400 and 2500 m. This plume likely originated from the Sea Cliff or other preexisting

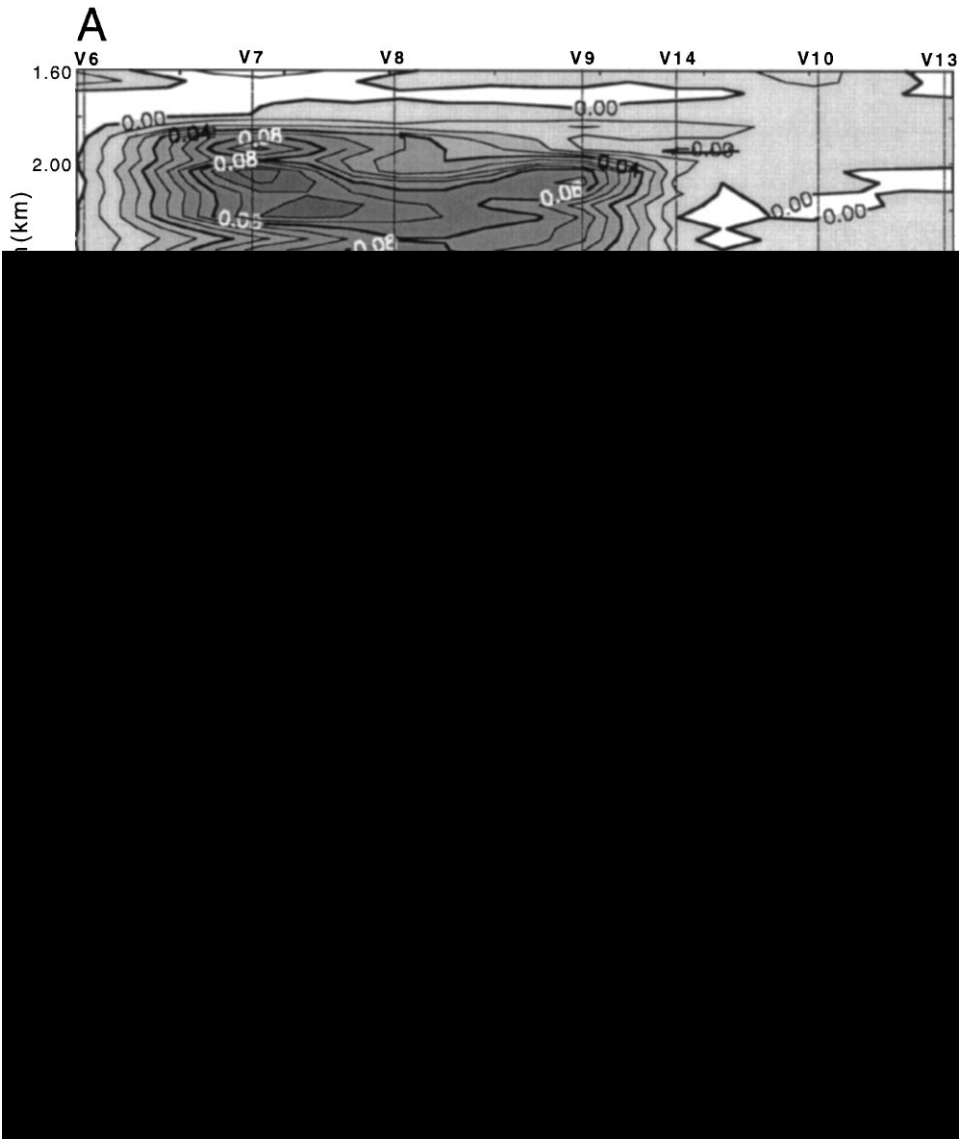

Fig. 3. Along-axis (A) and across-axis (B) temperature anomaly transects of EP96A from GR1. Complicated internal structure of EP96A suggests it was still forming during GR1. Darkened segments of bathymetry mark locations of mapped eruption centered at 42.67°N and suspected eruption at 42.61°N.

vent field. Ratios of $^{3}He/\Delta\theta$ in the plumes at both locations were $\sim 2.3 \times 10^{-12}$ cm^3 STP g^{-1} °C^{-1}, typical for established hydrothermal discharge but considerably higher than the standard value of ~ 0.3–0.4×10^{-12} cm^3 STP g^{-1} °C^{-1} found in all event plumes including EP96A (Lupton et al., 1989, 1995; Kelley et al., 1998).

Table 1
Event plume statistics

Event plume	Discovery date	Lat (°N)	Long (°W)	Min $\Delta\theta$ (°C)	Vol[a] (km^3)	f_θ	Max $\Delta\theta$ (°C)	Heat[a] (10^{15} J)	Rescaled[b] Heat (10^{15} J)	Lava[c] Heat (10^{15} J)
EP86A	20 Aug. 1986	44.8°	130.2°	0.01	149	2.17	0.28	89	193	253
EP87A	13 Sep. 1986	45.25°	130.2°	0.01	78	2.17	0.23	32	69	?
EP93A	11 Jul. 1993	46.53°	129.57°	0.005	15	2.17	0.25	4.1	8.9	
EP93B	11 Jul. 1993	46.47°	129.6°	0.005	34	2.17	0.20	10	22	40
EP93C	26 Jul. 1993	46.27°	129.62°	0.005	60	2.17	0.18	18	39	
EP96A	10 Mar 1993	42.63°	126.7°	0.01	128	2.43	0.12	21	51	83
EP96B	12 Apr 1993	42.7°	126.98°	0.005	69	2.43	0.069	5.1	12	46

[a]Volume and heat within the minimum $\Delta\theta$ contour mapped.
[b]Observed heat multiplied by the rescaling factor f_θ (Lavelle et al., 1998).
[c]Estimated total lava volume (Chadwick et al., 1998) multiplied by a heat capacity of $4.6 \times 10^9\ J\,m^{-3}$.

Moreover, there were no signs of mixing by lateral intrusions indicative of substantial erosion of EP96B. An alternative hypothesis is that EP96B was formed by the fractionation of EP96A caused by its inherent instability (cf. Helfrich and Battisti, 1991). In laboratory experiments (Helfrich and Battisti, 1991), simulated hydrothermal plumes became unstable when the radius exceeded $\sim$1 Rossby radius, Nz_m/f, where N is the buoyancy frequency, z_m is the height to the top of the plume spreading layer, and f is the Coriolis frequency. The physical radius of EP96A was greater than its Rossby radius of 5 km, so it was a candidate for fractionation into two or more smaller eddies. However, the association of EP96B with the southern chronic plume and eruption site, combined with differences in chemistry between EP96A and B (e.g. Cowen et al., 1998; Feely et al., 1998; Massoth et al., 1998), make the fractionation hypothesis less likely.

Over Gorda Ridge itself, three tows extending the length of the western, central, and eastern portions of the axial valley (Fig. 5C) found no evidence of significant plumes. A shorter tow directly along the trend of the northern lava mound found only occasional and weak ($< 0.015^\circ$C) temperature anomalies within 200 m of the seafloor. No plume from the hypothesized southern eruption site was detected. Chronic venting associated with the Gorda Ridge dike intrusion event thus produced organized plumes for no more than three months, much shorter than following dike intrusions on the CoAxial ($\sim$3 yr) (Baker et al., 1998) and Cleft (> 10 yr) (Baker, 1994, 1997) segments of the Juan de Fuca Ridge.

The rapid decline of hydrothermal activity associated with the Gorda Ridge eruption suggests that event and chronic plumes there depended almost exclusively on the dike intrusion for heat. This short time scale agrees at least qualitatively with a recent numerical model of dike cooling following intrusion into a cold, saturated porous layer (Cherkaoui et al., 1997). This model found that while the initial thermal decay at the CoAxial sites could be explained by cooling of a few-meters-wide dike extending about 500–2000 m below the seafloor, the lingering of measurable plumes 2–3 yr after the eruption demanded an additional heat source. Presumably, the dike intrusion at CoAxial opened up new fluid pathways to a region of hot rock at depth. The quicker quenching of hydrothermal plumes at the Gorda Ridge site suggests that no such pathways were created there.

4. Discussion

Since the 1986 discovery of the first event plume, EP86A, at the northern end of the Cleft segment on the JDFR (Baker et al., 1987a) six additional event plumes have been mapped over northeast Pacific spreading centers. EP86A can been ascribed to a volcanic eruption known to have occurred between 1983 and 1987 (Chadwick and Embley, 1994). A second event plume, EP87A, was found $\sim$50 km north of EP86A, but cannot be attributed to a specific seafloor event (Baker et al., 1989; Gendron et al., 1993). Three plumes, EP93A, B, and C, were associated with the 1993 eruption at the CoAxial segment of the JDFR (Baker et al., 1995). The two plumes described in this paper bring the total to seven. While all these plumes have strong similarities, they

have varied in size by over an order of magnitude (Table 1) and have been followed by very different histories of chronic venting. Comparison of these event plumes leads to new insights about their generation and subsequent aging.

4.1. Event plume aging

Because EP96A was sampled only in March, and EP96B was only poorly sampled in April, our ability to observe temporal changes within these event plumes is limited. Nevertheless, some new conclusions can be drawn about event plume duration and particle transport. Under the hypothesis that EP96B was released during the seismic swarm centered around 42.60°N from 10 to 20 March (and most likely during the most intense swarm on 16 March (Fox and Dziak, 1998), it was ~90 days old when rediscovered in early June. (Under the alternate hypothesis of Massoth et al. (1998) EP96B would have been ~60 days old in June). Three months after formation, EP96B showed no obvious indications of the kind of edge erosion by 1–100 m thick lateral thermohaline intrusions that eventually leads to the dissipation of subsurface, circular, long-lasting eddies typically found in the upper ocean (McWilliams, 1985), such as the well-studied though much larger "Meddies" in the northeast Atlantic (e.g. Armi et al., 1988).

Another question of interest is the capability of event plumes to maintain entrained particles in suspension, thereby providing a long-distance dispersal mechanism. Low and variable values of the optical/$\Delta\theta$ ratio are characteristic of very young event plumes. Short-period time-series sampling of the CoAxial event plume EP93A demonstrated that the optical/$\Delta\theta$ ratio increased for at least 3 days before reaching a steady value, a trend that reflects the phase change of Fe from dissolved (i.e. passes through a 0.4 μm pore filter) to particulate form, as well as particle aggregation (Baker et al., 1995; Massoth et al., 1995; Massoth et al., 1998). Comparison of the optical/$\Delta\theta$ ratio in many event plumes shows that all mature event plumes reach an equilibrium value quite uniform within a given plume and remarkably similar between plumes. For example, EP86A and EP96B both had a $\Delta n/\Delta\theta$ ratio of ~0.8 V °C^{-1}, and EP93B and EP96A a ratio of ~0.56, although both these latter plumes contained parcels of presumably younger plume fluids with even lower ratios (Fig. 6). The youngest event plume yet sampled appears to have been EP93A, much of which had a $\Delta n/\Delta\theta$ ratio < 0.08 V °C^{-1}. The difference in $\Delta n/\Delta\theta$ ratios between EP96A and B is additional evidence that these plumes were formed independently. Moreover, the identical ratios of EP96B in April and June indicates that no measurable loss of particles (or at least no change in their light-scattering response) occurred between GR2 and 3. An alternate, but less plausible, explanation is that particle production within EP96B exactly balanced particle loss by dissolution and sinking.

4.2. Event plume generation

While the Cleft, CoAxial, and Gorda Ridge events have each begun with a near-simultaneous eruption of lava and event plume(s), the subsequent discharge history at each site has differed materially. Any explanation of the hydrothermal activity

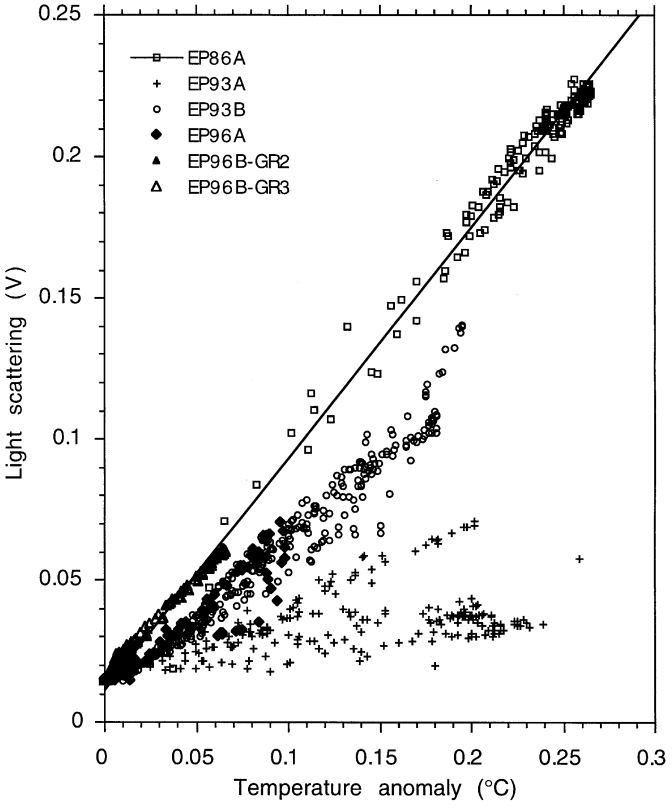

Fig. 6. Scatter plot of relative light scattering vs. temperature anomaly for five event plumes. Optical data from EP87A were compromised by transmissometer drift; data are unavailable from EP93C owing to transmissometer failure. Original optical data for EP86A, EP93A, and EP93B were from a beam transmissometer and have been converted to light scattering using equation (2). Mature event plumes have a highly uniform $\Delta n/\Delta\theta$ ratio. For EP86A, EP96B-GR2, and EP96B-GR3 the ratio was ~ 0.8 V°C^{-1}. The ratio was lower and more variable for younger plumes EP93B and EP96A(~ 0.56 V°C^{-1}), and much lower and highly variable for the very young plume EP93A. The EP93A ratio rose to the level of EP93B within about 5 days (Baker et al., 1995). The maximum value of the ratio for a given event plume presumably can vary depending on the particle load, which is dominated by iron oxides (Massoth et al., 1995).

associated with intrusion events must account for several specific physical observations (plus chemical and biological constraints not discussed here).

(1) *The discharge of heat and mass declines precipitately following an intrusion* (Fig. 7). This decline was first quantified at the CoAxial site, where frequent plume advection measurements at the Flow and Floc vent fields showed that the total heat flux decreased over time t as a power curve, t^{-k}, with $k \approx 0.8$ (Baker et al., 1998). This rate is somewhat higher than that expected from a standard conductive cooling curve ($t^{-1/2}$), assuming the transfer of heat to vent fluids occurs by conductive cooling of hot rock (Lowell and Rona, 1985). The discrepancy suggests that other physical properties

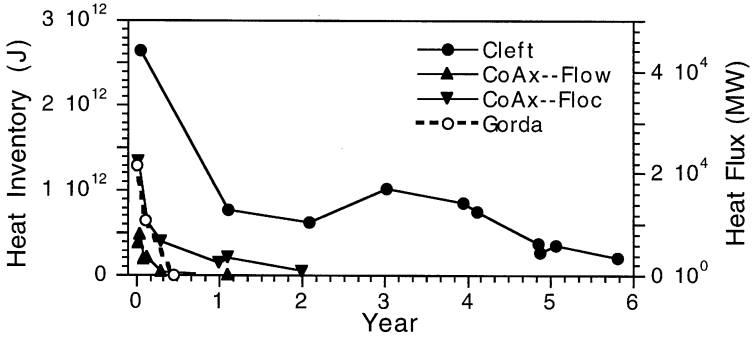

Fig. 7. Trend of chronic plume heat inventory vs. time after eruption perturbation for four sites. Q (J) is the hydrothermal heat contained in a 1 m thick along-axis slice of plume. H (MW) is the heat flux calculated from plume advection measurements, valid only for the two CoAxial sites (Baker et al., 1998). Q at time zero for the Gorda Ridge eruption is unknown and is assumed to be approximately twice the value at 0.1 yr, based on the CoAxial results. The Cleft trend was apparently perturbed by a second eruption in year three, as indicated by an increase in the ^{3}He/heat ratios of the chronic plume (Massoth et al., 1994).

besides conductive cooling affect the heat transfer. Possibilities include permeability, dike thickness, the thickness of the permeable layer into which the dike intrudes, and other factors (Cherkaoui et al., 1997). While flux calculations have not been made at the Cleft or Gorda Ridge sites, the trend of plume heat inventories at these sites suggests a similar pattern of rapid decline (Fig. 7). Note that the trend at the Cleft site was complicated apparently by a second event in 1989, when both the heat content (Baker, 1994) and ^{3}He/heat ratios (Massoth et al., 1994) in the chronic plume increased.

(2) *The time scale of the post-intrusion decline varies widely, both among and within sites* (Fig. 7). Whereas organized hydrothermal discharge at the Gorda Ridge site lasted no more than three months, substantial plumes remain at the Cleft site 10 years after the 1986 event plume. At CoAxial, venting at the eruption location (Flow) declined much faster than at the Floc site about 30 km upstrike from the eruption. Cleft may also exhibit a similar trend. Active venting at Cleft now occurs almost exclusively upstrike from a series of lava pillow mounds thought to be contemporaneous with the 1986 event plume (Chadwick et al., 1991; Embley et al., 1991; Baker, 1994). The mounds themselves were not visited by camera or submersible until 1989–91, and by then only isolated pockets of low-temperature diffuse venting were found (Chadwick and Embley, 1994). A brief episode of high-temperature discharge there could easily have gone undetected.

(3) *Event plumes may form in as little as a few hours, and the discharge of multiple event plumes during an intrusion is commonplace.* Simulations using a three-dimensional non-hydrostatic hydrodynamical model indicate that 350°C fluids exiting from a line source of length $\sim$1 km could form an EP96A-sized event plume in only a few hours (Lavelle, 1995). If event plume heat is mined from a dike or lava flow, the heat transfer must be remarkably rapid. If lava cooling is the principal heat source, then

multiple event plumes necessitate multiple eruption episodes and these episodes must each hold sufficient heat to supply the event plumes. Table 1 compares the total latent and specific heat supplied by basaltic lava solidification and cooling from 1100°C to 0°C (4.6×10^9 J m^{-3}) at each event plume site with the heat contained in event plumes. The observed heat inventory is corrected by a rescaling factor, f_θ, which can be applied to volume integrals of $\Delta\theta$ anomalies calculated according to equation (1) to yield total source heat flux for event plumes (Lavelle et al., 1998). This comparison indicates that event plumes would have required most or all of the available heat in the extruded lava at each site, thus demanding almost total extrusion and cooling within a few hours. For this reason, production of event plumes solely from cooling lava seems unlikely.

The same analysis is not easily applied to dike cooling, as the available surface area and volume are unknown. Regardless of what mechanism may produce event plumes from within the crust—by dike cooling (Lowell and Germanovich, 1995), release of magmatic fluids (Nehlig, 1993), or fluid expansion (Wilcock, 1997), for example—successful models must accommodate multiple episodes separated in time and/or space to liberate successive event plumes.

(4) *The presence of an existing high-temperature vent field may not be necessary or even conducive to event plume formation.* None of the three event sites discussed here had been surveyed immediately before the event, but at both CoAxial (Baker et al., 1998) and Gorda the available data suggest an absence of vigorous venting some years before the event. Only at the site of the 1991 eruption near 9.8°N on the East Pacific Rise is there concrete evidence for preexisting high-temperature discharge (Haymon et al., 1993). And at the EPR site, eight CTD profiles between 9.8° and 9.5°N taken within days of the eruption found no evidence of event plumes over the ridge axis (Macdonald et al., 1992).

(5) *The ratio of total chronic to event discharge varies markedly among intrusion events.* This variation may be a function of the crustal structure at a given eruption site. Quantitative studies of discharge following the CoAxial eruption have concluded that event plumes accounted for $< 5\%$ of the total heat emitted during the lifetime of the Flow and Floc vent fields (Baker et al., 1998). While our knowledge about chronic discharge following the Cleft and Gorda eruptions is less quantitative, the trends illustrated in Fig. 7, combined with estimated inventories of the event plume heat at each site (Table 1), suggest that the ratio of chronic to event plume heat discharge was roughly similar (or perhaps greater) at Cleft but far smaller at Gorda. At the EPR, chronic discharge remains vigorous a full five years after the 1991 eruption (Von Damm et al., 1995; K. Von Damm and M. Lilley, pers. comm.), although no vent-field-scale measurements of total heat flux have been made. A substantial chronic flux, combined with the apparent absence of event plumes, implies a very high ratio of chronic to event plume discharge relative to the northeast Pacific sites. These observations suggest that eruptions on ridge segments where the partial melt horizon is relatively shallow and the volume of the hydrothermal reaction zone in the crust consequently is small (e.g. the EPR) will produce small or no event plumes but long-lasting chronic plumes. Conversely, eruptions on segments where melt lies deep below or distant from the eruption site (e.g. Gorda Ridge) may produce large event plumes but only ephemeral chronic plumes if no fluid pathways to more substantial

heat sources are created. Alternatively, this inter-site variability may arise from substantial differences in the local permeability structure.

Development of testable models from these observations will require not only additional response efforts but at least occasional responses involving a measurement suite both broader and denser than has been possible to date. At minimum must be the basic measurements common to most previous event responses: identification of lava eruptions and quantification of their volumes, a comprehensive search for event plumes, and time-series sampling of chronic plumes. Most acutely needed to materially improve our understanding of the origin of event plumes and their relationship to chronic hydrothermal discharge is improved passive and active seismic investigation, especially an early and extensive deployment of seafloor seismometers or hydrophones. Such an improvement will require a commitment either to stockpile and deploy geophysical instrumentation as part of an immediate response effort, or to sustain a comprehensive ridge seafloor observatory at a site judged likely to experience an intrusion.

Acknowledgements

This research was supported by the NOAA VENTS Program. Expeditious funding by the Ocean Sciences Division of NSF provided the UNOLS ship *Wecoma* for the GR2 cruise, admirably organized and run by Chief Scientist J. Cowen and co-Chief Scientist R. Embley. Thanks to S. L. Walker for CTD processing and operational help on GR1 and 3, to C. Wilson for CTD help on GR2, and a variety of colleagues on GR1, 2, and 3 who helped keep the CTD running. Contribution number 1848 from the NOAA/Pacific Marine Environmental Laboratory.

References

Armi, L., Herbert, D., Oakey, N., Price, J., Richardson, P.L., Rossby, T., Ruddick, B., 1988. The history and decay of a Mediterranean salt lens. Nature 333, 649–651.

Baker, E.T. 1994. A six-year time series of hydrothermal plumes over the Cleft segment of the Juan de Fuca Ridge. Journal of Geophysical Research 99, 4889–4904.

Baker, E.T. 1997. Long-term monitoring of hydrothermal discharge by means of plume surveys: Results from the first decade and questions for the next. EOS Transactions of the American Geophysical Union 78, 46 (Fall Meet. Suppl., F756).

Baker, E.T., Massoth, G.J., Feely, R.A. 1987a. Cataclysmic hydrothermal venting on the Juan de Fuca Ridge. Nature 329, 149–151.

Baker, E.T., Massoth, G.J., Collier, R.W., Trefry, J.H., Kadko, D., Nelsen, T.A., Rona, P.A., Lupton, J.E., 1987b. Evidence for high-temperature hydrothermal venting on the Gorda Ridge, Northeast Pacific Ocean. Deep-Sea Research 34, 1461–1476.

Baker, E.T., Lavelle, J.W., Feely, R.A., Massoth, G.J., Walker, S.L., Lupton, J.E., 1989. Episodic venting of hydrothermal fluids from the Juan de Fuca Ridge. Journal of Geophysical Research 94, 9237–9250.

Baker, E.T., Massoth, G.J., Feely, R.A., Embley, R.W., Thomson, R.E., Burd, B.J., 1995. Hydrothermal event plumes from the CoAxial seafloor eruption site, Juan de Fuca Ridge. Geophysical Research Letters 22, 147–150.

Baker, E.T., Urabe, T., 1996. Extensive distribution of hydrothermal plumes along the superfast-spreading East Pacific Rise, 13°50N′–18°40′S. Journal of Geophysical Research 101, 8685–8695.

Baker, E.T., Massoth, G.J., Feely, R.A., Cannon, G.A., Thomson, R.E., 1998, The rise and fall of the CoAxial hydrothermal site, 1993–1996. Journal of Geophysical Research 103, 9791–9806.

Chadwick, Jr., W.W., Embley, R.W., Fox, C.G., 1991. Evidence for volcanic eruption on the southern Juan de Fuca Ridge between 1981 and 1987. Nature 313, 212–214.

Chadwick, Jr., W.W. Embley, R.W. 1994. Lava flows from a mid-1980s submarine eruption on the Cleft segment, Juan de Fuca Ridge. Journal of Geophysical Research 99, 4761–4776.

Chadwick Jr, W.W., Embley, R.W., Fox, C.G., 1995. Sea Beam depth changes associated with recent lava flows, CoAxial segment, Juan de Fuca Ridge: Evidence for multiple eruptions between 1981–1993. Geophysical Research Letters 22, 167–170.

Chadwick, Jr., W.W., Embley, R.W., Shank, T., 1998. The 1996 Gorda Ridge eruption: Geologic mapping, sidescan sonar, and SeaBeam comparison results. Deep-Sea Research II 45, 2547–2569.

Cherkaoui, A.S.M., Wilcock, W.S.D., Baker, E.T., 1998. Thermal fluxes associated with the 1993 diking event on the CoAxial segment, Juan de Fuca Ridge: A model for the convective cooling of a dike. Journal of Geophysial Research 102, 24 887–24 902.

Collier, R.W., Baker, E.T., 1990. Hydrography and geochemistry of northern Gorda Ridge. In: McMurray, G.R. (Ed.), Gorda Ridge, A seafloor spreading center in the United States' Exclusive Economic Zone. Springer, New York, pp. 21–30.

Cowen, J.P., Bertram, M.A., Baker, E.T., Massoth, G.J., Feely, R.A., Summit, M. 1998. Geomicrobial transformation of manganese in Gorda Ridge event plumes. Deep-Sea Research II 45, 2713–2737.

Davis, J.C. 1987. Contour mapping and SURFACE III. Science 237, 669–672.

Dziak, R.P., Fox, D.G., Schreiner, A.E., 1995. The June–July 1993 seismo-acoustic event at CoAxial segment, Juan de Fuca Ridge: Evidence for a lateral dike injection. Geophys. Res. Lett. 22, 135–138.

Embley, R.W., Chadwick, W., Perfit, M.R., Baker, E.T., 1991. Geology of the northern Cleft segment, Juan de Fuca Ridge: Recent lava flows, sea-floor spreading, and the formation of megaplumes. Geology 19, 771–775.

Feely, R.A., Baker, E.T., Lebon, G.T., Gendron, J.F., Massoth, G.J., Mordy, C., 1998. Chemical variations of hydrothermal particles in the 1996 Gorda Ridge event and chronic plumes. Deep-Sea Research II 45, 2637–2664.

Fox, C.G., Radford, W.E., Dziak, R.P., Lau, T.-K., Matsumoto, H., Schreiner, A.E., 1995. Acoustic detection of a seafloor spreading episode on the Juan de Fuca Ridge using military hydrophone arrays. Geophysical Research Letters 22, 131–134.

Fox, C.G., Dziak, R.P., 1998. Hydroacoustic detection of volcanic activity on the Gorda Ridge, February–March, 1996. Deep-Sea Research II 45, 2513–2530.

Gendron, J.F., Cowen, J.P., Feely, R.A., Baker, E.T., 1993. Age estimate for the 1987 megaplume on the southern Juan de Fuca Ridge using excess radon and manganese partitioning. Deep-Sea Research 40, 1559–1567.

Haymon, R.M., Fornari, D.J., Von Damm, K.L., Lilley, M.D., Perfit, M.R., Edmond, J.M., Shanks, W.C., III, Lutz, R.A., Grebmeier, J.M., Carbotte, S., Wright, D., McLaughlin, E., Smith, M., Beedle, N., Olson, E., 1993. Volcanic eruption of the mid-ocean ridge along the East Pacific Rise at 9°45–52′N: direct submersible observations of seafloor phenomena associated with an eruption event in April, 1991. Earth and Planetary Science Letters 119, 85–101.

Helfrich, K.R., Battisti, T.M., 1991. Experiments on baroclinic vortex shedding from hydrothermal plumes. Journal of Geophysical Research 96, 12 511–12 518.

Kelley, D.S., Lilley, M.D., Lupton, J.E., Olson, E.J., 1998. Enriched H_2, CH_4, and ^3He concentrations in hydrothermal plumes associated with the 1996 Gorda Ridge eruptive event. Deep-Sea Research II 45, 2665–2682.

Lavelle, J.W., 1995. The initial rise of a hydrothermal plume from a line segment source—results from a three-dimensional numerical model. Geophysical Research Letters 22, 159–162.

Lavelle, J.W., Baker, E.T., Massoth, G.J., 1998. On the calculation of total heat, salt and tracer fluxes from ocean hydrothermal events. Deep-Sea Research II 45, 2619–2636.

Lowell, R.P., Germanovich, L.N., 1995. Dike injection and the formation of megaplumes at ocean ridges. Science 267, 1804–1807.

Lowell, R.P., Rona, P.A., 1985. Hydrothermal models for the generation of massive sulfide ore deposits. Journal Geophysical Research 90, 8769–8783.

Lupton, J.E., Baker, E.T., Massoth, G.J., 1989. Variable 3He/heat ratios in submarine hydrothermal systems: evidence from two plumes over the Juan de Fuca Ridge. Nature 337, 161–164.

Lupton, J.E., Baker, E.T., Massoth, G.J., Thomson, R.E., Burd, B.J., Butterfield, D.F., Embley, R.W., Cannon, G.A., 1995. Variations in water-column ^{3}He/heat ratios associated with the 1993 CoAxial event, Juan de Fuca Ridge. Geophysical Research Letters 22, 155–158.

Lupton, J.E., Baker, E.T., Garfield, N., Massoth, G., Feely, R., Cowen, J., Greene, R., Rago, T., 1998. Tracking the evolution of a hydrothermal event plume using a RAFOS neutrally bouyant drifter. Science 280, 1052–1055.

Macdonald, K.C., Baker, E.T., Haymon, R., Lilley, M.D., Perfit, M.R., Fornari, D.J., Von Damm, K., 1992. Time-series water column measurements and submersible observations at EPR 9°30′N–10°02′N from 4/91 to 3/92: Evidence for changing hydrothermal activity. EOS Transactions of the American Geophysical Union 73 (Fall Suppl.) 530.

Massoth, G.J., Baker, E.T., Lupton, J.E., Feely, R.A., Butterfield, D.A., Von Damm, K., Roe, K.K., Lebon, G.T., 1994. Temporal and spatial variability of hydrothermal manganese and iron at Cleft segment, Juan de Fuca Ridge. Journal of Geophysical Research 99, 4905–4923.

Massoth, G.J., Baker, E.T., Feely, R.A., Butterfield, D.A., Embley, R.E., Lupton, J.E., Thomson, R.E., Cannon, G.A., 1995. Observations of manganese and iron at the CoAxial seafloor eruption site, Juan de Fuca Ridge. Geophysical Research Letters 22, 151–154.

Massoth, G.J., Baker, E.T., Feely, R.A., Lupton, J.E., Collier, R.W., Gendron, J.F., Roe, K.K., Maenner, S.M., Resing, J.A., 1998. Manganese and iron in hydrothermal plumes resulting from the 1996 Gorda Ridge Event. Deep-Sea Research II 45, 2683–2712.

McWilliams, J.C., 1985. Submesoscale, coherent vortices in the ocean. Review Geophysics 23, 165–182.

Nehlig, P., 1993. Interactions between magma chambers and hydrothermal systems: oceanic and ophiolitic constraints. Journal of Geophysical Research 98, 19 621–19 633.

Riddihough, R.P., 1980. Gorda plate motions from magnetic anomaly analysis. Earth and Planetary Science Letters 51, 163–170.

Rona, P.A., Delinger, R.P., Fisk, M.R., Howard, K.J., Taghon, G.L., Klitgord, K.D., McClain, J.S., McMurray, G.R., Wiltshire, J.C., 1990. Major off-axis hydrothermal activity on the northern Gorda Ridge. Geology 18, 493–406.

Von Damm, K.L., Oosting, S.E., Kozlowski, R., Buttermore, L.G., Colodner, D.C., Edmonds, H.N., Edmond, J.M., Gregmeier, J.M., 1995. Evolution of East Pacific Rise hydrothermal vent fluids following a volcanic eruption. Nature 375, 47–50.

Wilcock, W.S.D., 1997. A model for the formation of transient plumes above mid-ocean ridge hydrothermal systems. Journal of Geophysical Research 102, 12 109–12 121.